Synthesis and Characterization of NMC 811 by Oxalate and Hydroxide Coprecipitation Method

Himmah Sekar Eka Ayu Gustiana
Chemical Engineering Department, Faculty of Vocational Studies, Universitas Sebelas Maret

Firda Reza Agustiana
Department of Physics Faculty of Mathematics and Natural Science, Universitas Sebelas Maret

Shofirul Sholikhatun Nisa
Centre of Excellence for Electrical Energy Storage Technology, Universitas Sebelas Maret

Endah Retno Dyartanti
Centre of Excellence for Electrical Energy Storage Technology, Universitas Sebelas Maret

https://doi.org/10.5109/4794169

出版情報：Evergreen. 9 (2), pp.438-442, 2022-06. 九州大学グリーンテクノロジー研究教育センター
バージョン：

Synthesis and Characterization of NMC 811 by Oxalate and Hydroxide Coprecipitation Method

Himmah Sekar Eka Ayu Gustiana[1,3], Firda Reza Agustiana[2], Shofirul Sholikhatun Nisa[3], and Endah Retno Dyartanti[3,4,*]

[1]Chemical Engineering Department, Faculty of Vocational Studies, Universitas Sebelas Maret, Jl. Kolonel Su tarto No. 150K, Surakarta, Central Java 57126, Indonesia

[2]Department of Physics Faculty of Mathematics and Natural Science, Universitas Sebelas Maret, Jl. Ir. Suta mi No. 36A, Surakarta, Central Java 57126, Indonesia

[3]Centre of Excellence for Electrical Energy Storage Technology, Universitas Sebelas Maret, Jl. Slamet Riyad i No. 435, Surakarta, Central Java 57146, Indonesia

[4]Chemical Engineering Department, Faculty of Engineering, Universitas Sebelas Maret, Jl. Ir. Sutami No. 36 A, Surakarta, Central Java 57126, Indonesia

*Author to whom correspondence should be addressed:
E-mail: endah_rd@staff.uns.ac.id

(Received December 7, 2021; Revised June 3, 2022; accepted June 3, 2022).

Abstract: Synthesis of $LiNi_{0.8}Mn_{0.1}Co_{0.1}O_2$ (NMC 811) by coprecipitation method is promising for use. In this study, different precipitation agents were used to comparing the characterization of each cathode. XRD analysis shows that both samples of NMC 811 have a highly layered hexagonal structure. By using FTIR analysis, it was indicated that the two cathodes contain C-H, O-H and C-O groups. Based on SEM analysis, the constituent particles of the cathodes are spherical asymmetrical with the size of the primary particle less than 1 micron and for the secondary particle more than 1 micron. The electrochemical performance showed that NMC-oxalate has a higher specific capacity than NMC-hydroxide. Based on this analysis, oxalate gave better results than hydroxide as a precipitate agent.

Keywords: Lithium-ion battery; NMC 811; coprecipitation

1. Introduction

Battery, an energy storage device in an electrochemical cell, can directly convert chemical energy into electrical energy. Until now, they have been widely used in many electronic devices. When the battery is used, it must be able to work efficiently, effortlessly, environment-friendly and high capacity[1–3]. One of the efficient batteries is a secondary battery such as a Li-ion battery[4–7]. The reaction that occurs in the secondary battery is reversible. When the battery is used by connecting the load to the battery terminals (discharge), electrons flow from the negative terminal to the positive, resulting in battery charging[8]. In comparison to other secondary batteries, Li-ion batteries have a longer lifespan (500-2000 cycles), alongside a higher energy density and capacity[1,4,6].

Indonesia is one of the countries with the largest nickel in the world. Therefore, Indonesia has the potential to compete globally in producing nickel-based cathode materials. The nickel-based cathode materials are NMC (Lithium Nickel Manganese Cobalt Oxide) and NCA (Lithium Nickel Cobalt Aluminum Oxide). Of the two cathodes, NMC has advantages in specific capacity and stability structure[9]. Some Ni:Co:Mn compositions in the NMC cathode are 1:1:1, 5:3:2, 6:2:2 and 8:1:1. This study uses NMC 8:1:1 because it has a larger capacity[10–12]. In the future, from 2025 and beyond, research is expected to focus on the generation of battery cathode materials that can be applied in the automotive industry.

Several methods for processing NMC are sol-gel, coprecipitation, hydrothermal and solid-state[6,13]. In this study, $LiNi_{0.8}Mn_{0.1}Co_{0.1}O_2$ (NMC 811) was synthesized using the coprecipitation method. This method is very simple and the process involves controlling pH, temperature and stirring speed. Nevertheless, characterization of the NMC 811 cathode depends on the precipitating agent used[14]. Commonly, oxalate and hydroxide are precipitating agents that are often used to synthesize of battery cathodes by the coprecipitation method[13,15,16]. The oxalate ion in the solution serves as both a precipitating and a complexing agent in oxalate

coprecipitation. The formation of metal complexes reduces the rate of deposition and allows for more controlled nucleation and particle growth. Furthermore, most ternary metals employed in cathode materials, such as Ni, Co, Mn, and their combinations, generate stable oxalate dihydrates over the whole mixing ratio range. Meanwhile, hydroxide coprecipitation can result in homogeneous mixing of cations and monodispersions related to particle shape and particle size distribution[17].

NMC 811 was synthesized by coprecipitation method, using two different precipitating agents: sodium hydroxide and oxalic acid with the same synthesis conditions. These two precipitating agents have often been used and are easy to find commercially. However, so far, these two precipitants have not been directly compared for the precursor NMC 811. In this research, the effects of the different precipitating agents on morphology, structure and performance analysis of the cathode were studied to obtain the chemical fundamentals to produce a cathode with high capacity.

2. Experimental

0.8 moles of $NiCl_2.6H_2O$ (Zenith, Brazil), 0.1 moles of $CoSO_4.7H_2O$ (Rubamin, India) and 0.1 moles of $MnSO_4.H_2O$ (Jiayi Sunway Chem., China) were dissolved in 1 liter of aquadest. The precipitation agents used are sodium hydroxide (Asahi, Japan) and oxalic acid (Yuanping Changyuan, China).

NMC 811 solution was mixed with each precipitating agent for 2 hours at 60ºC and 4 hours of aging. NMC 811 uses sodium hydroxide (NMC-hydroxide) and oxalic acid (NMC-oxalate) as precipitating agents were synthesized using the mixture of each precursor and $LiOH.H_2O$ (Leverton) (1:1.05) by calcining at 450ºC for 6 hours in the furnace and sintering at 800ºC for 15 hours under flowing O_2. After that, the samples were analyzed using X-Ray Diffractometer (XRD) EQ-MD-10-LD Mini Diffractometer, MTI; Fourier Transform Infra-Red (FTIR) Shimadzu, Japan and Scanning Electron Microscope (SEM) JSM-6510LA, JEOL, Japan.

Cathodes were prepared by coating the slurry, consisting of active materials, acetylene black (AB) (MTI, USA) and polyvinylidene fluoride (PVDF) (MTI, USA) binder in N-methyl-2-pyrrolidone (NMP) (MTI, USA) solvent, onto an aluminum foil, followed by drying in the oven. After the electrode was completely dried, cells were assembled by filling 1M LiPF6 electrolyte in the glove box and tested in the battery analyzer.

3. Results and Discussion

3.1 Crystal structure analysis on XRD

Based on the results of the X-ray diffraction pattern, qualitative analysis was carried out with phase identification based on the adjustment of peak data with existing commercial databases. NMC-oxalate and NMC-hydroxide were adjusted to the existing commercial NMC 811 database.

As shown in Fig. 1, NMC-oxalate and NMC-hydroxide have eight peaks identical to commercial NMC 811. There are four significant peaks in each precipitating agent. NMC-oxalate at 19.64º, 36.86º, 44.65º and 64.73º, while NMC-hydroxide at 19.72º, 36.94º, 44.79º and 64.99º. In the commercial NMC 811 graph, the diffraction peak is obtained lattice parameters. The first peak shows (003) as a lattice parameter with 2θ of 19.47º. The second peak has lattice parameters of (101) and 2θ of 36.5º. The third peak has two lattice parameters of (006) / (012) because there are overlapping peaks at 2θ of 38.15º. The fourth peak, the highest intensity peak, has lattice parameters of (104) and 2θ of 44.38º. In the other peaks, each has lattice parameters of (105), (107), (108) / (110) and (113). While each of them, has 2θ of 48.55º, 58.58º, 64.76º and 68.23º. Then in Fig. 1, the 2θ values of NMC-oxalate and NMC-hydroxide were not much different from that of commercial NMC 811. From the XRD results, it can be concluded that the synthesis of NMC-oxalate and NMC-hydroxide was successfully carried out without detecting the secondary phase. NMC-oxalate dan NMC-hydroxide are totally into the oxide or free from impurities[16,18]. From lattice parameters of NMC 811 commercial, NMC-oxalate and NMC-hydroxide are synthesized by the coprecipitation method obtained a hexagonal structure[18,19]. It is indicated that the stoichiometry phase exchange of $Ni_{0.8}Mn_{0.1}Co_{0.1}$ and Li was fixed from the target[20].

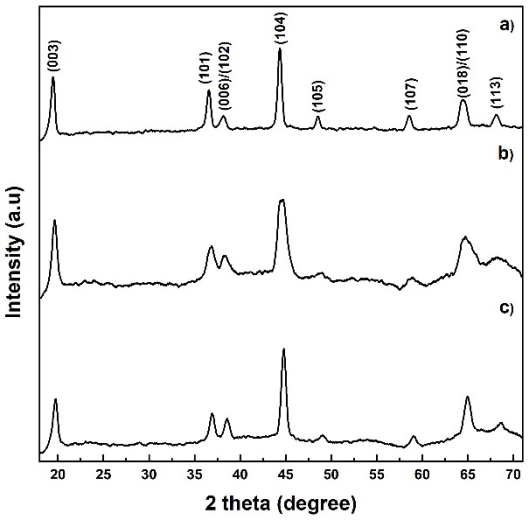

Fig. 1: Graph of diffraction peak analysis of: (a) commercial NMC 811, (b) NMC-oxalate, and (c) NMC-hydroxide

The lattice parameter (c/a) and crystal diameter (nm) provided in Table 1 were determined based on the examination of diffraction peaks and lattice parameters (hkl). According to the result, c/a lattice parameter's value was a direct measurement of the ideal cubic close-packed lattice and was valued at 4.90. This is significant because a structure with a c/a value greater than the stipulated value will become more regular and the lithium-ion

exchange will be easier[21,22]. Commercial NMC 811 has c/a of 4.93, while the c/a value of NMC 811 with oxalate and hydroxide precipitating agent can be seen in Table 1. It can be concluded that the two samples of NMC 811 synthesized by coprecipitation have a high layered material structure and easy lithium ion exchange properties.

Table 1. Lattice parameter (c/a) and crystal diameter of NMC 811

Sample	a (Å)	c (Å)	c/a	D (nm)
NMC-oxalate	2.87	13.99	4.89	177.83
NMC-hydroxide	2.85	13.98	4.90	155.86

3.2 FTIR analysis

Fig. 2 shows the results of FTIR analysis of NMC-oxalate and NMC-hydroxide, both precursor and cathode material products. In the NMC-oxalate precursor (Fig. 2a), there are O-H and C=O peaks at wave numbers 3406/cm and 1749/cm. There are C-O groups at wave numbers 1318/cm and 774/cm. Meanwhile, the wavenumber of 448/cm shows the metal-O group. NMC-oxalate precursor (containing C-O, O-H and metal-O functional groups) was calcined and sintered into NMC-oxalate product with the constituent groups being O-H and C-O. NMC-hydroxide precursor (Fig. 2b) has the similar functional group as NMC-oxalate. The O-H and C=O group is found at 3614/cm and 1644/cm, and the C-O group is at 1320/cm and 1098/cm. A metal-O group was found at a wavenumber of 497/cm. NMC-hydroxide precursor (containing C-O, O-H and metal-O) was calcined and sintered into NMC-hydroxide product (containing C-H, O-H and C-H). It can be seen that the two products have the same constituent groups, which are O-H and C-O groups. These results are in agreement with the data reported by Nisa, et al.[23] and Ubaidullah, et al[24].

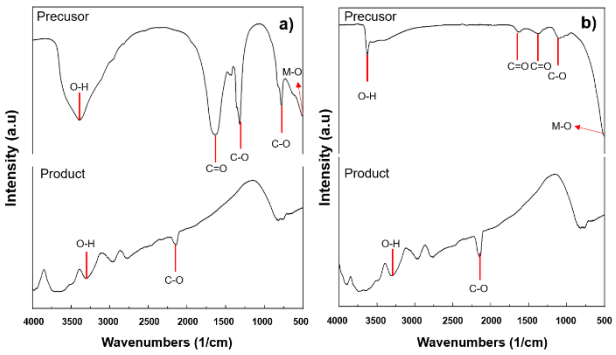

Fig. 2: FTIR characterization of (a) NMC-oxalate, (b) NMC-oxalate and NMC-hydroxide

3.3 SEM analysis

Fig. 3a shows that SEM analysis of NMC-oxalate obtained a slightly elongated spherical morphology. The average size of secondary particles of it is 4.95 µm and primary particles are 0.62 µm. Besides that, SEM analysis of NMC-hydroxide revealed an asymmetric spherical morphology (Fig. 3b). The average size of the secondary particles is 3.19 µm and primary particles are 0.73 µm. The constituent particles of NMC 811 are spherical asymmetrical with a primary particle size of less than 1 µm and secondary particles of more than 1 µm[25]. Smaller particles can reduce Li^+ ion diffusion distances and enhance surface contact area between the electrode and the electrolyte. As a result of the reduced particle size, increased specific capacity and level performance will be possible[15]. However, smaller particles can facilitate the formation of a solid electrolyte interface (SEI) as a result of undesirable electrode/electrolyte interactions, resulting in self-discharge and inefficient cycling[26].

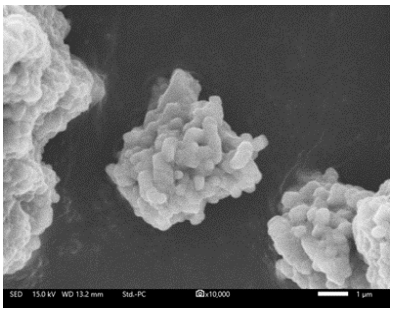

(a)

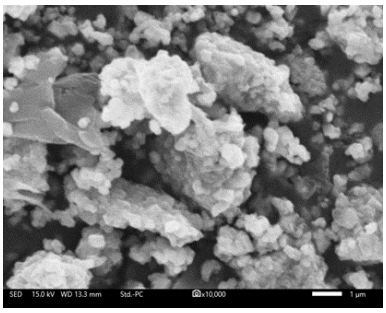

(b)

Fig. 3: Characterization SEM of (a) NMC-oxalate and (b) NMC-hydroxide at 10,000x magnification.

3.4 Battery performance analysis

A significant upward curve shown in Fig. 4 indicates the battery is charging, while a significant downward curve shows the battery discharge. From this process, the battery cells capacity can be determined. The capacity of battery cell is the amount of electrical energy that the battery can issue at a certain time. The capacity of this battery depends on the type of active material used and the speed of the electrochemical reaction when the battery is charged or discharged. The extent of surface contact between active materials affects the increase in battery capacity[27].

Fig. 4 shows the MPV (MidPoint Voltage) and EODV (End of Discharge Voltage) areas in the battery performance analysis with charge-discharge testing. MPV area is the nominal cell voltage at the voltage measured

when the battery has discharged 50% of the total energy. While the area of EODV is the cell voltage measured at the end of the operating period. The cathode of the coprecipitation method, which has a higher battery capacity, is NMC-oxalate. This is shown in Fig. 4, where the specific capacity of NMC-oxalate is 102.42 mAh/g while NMC-hydroxide has a specific capacity of 79.90 mAh/g. NMC-oxalate has a higher capacity because it has slightly larger particles and a more regular morphology than NMC-hydroxide. As previously mentioned, the smaller particles facilitate the formation of SEI, although both have similar XRD and FTIR analysis results. Another study reported a specific capacity of NMC 811 is achieved up to 231.50 mAh/g vs. Li/Li^{+}[28].

From the charge-discharge test can obtain the value of efficient coulomb. Coulombic efficiency can be calculated by the capacity at discharge divided by the capacity at a charge. The value of coulombic efficiency for NMC oxalate is 104% and NMC hydroxide is 97%. Coulombic efficiency describes the ratio between the charge into and out of the battery in a cycle. A good value of coulombic efficiency if the value is above 80% and increases when charging quickly can prove that the battery system is stable[19,29].

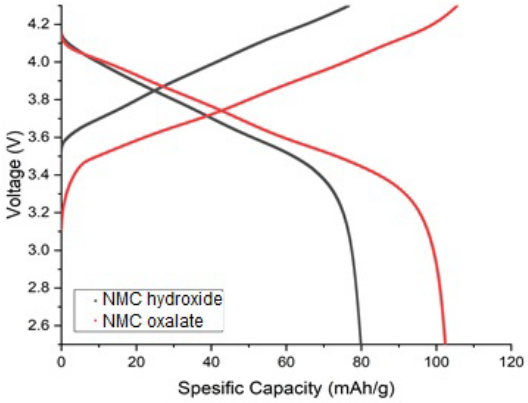

Fig. 4: Battery performance analysis with charge-discharge test at 0.1 C

4. Conclusion

In this study, NMC 811 was successfully synthesized using the coprecipitation method with oxalic acid and sodium hydroxide. NMC-oxalate and NMC-hydroxide have structural characteristics of layered material with a hexagonal shape identical to the structure in the R_3m space group with a good atomic arrangement. NMC-oxalate and NMC-hydroxide are composed of C-H, O-H and C-O functional groups. They have micron size but different morphological characters. The battery capacity of the NMC oxalate is 102.42 mAh/g and the NMC hydroxide is 79.90 mAh/g in the charge-discharge battery test using the battery analyzer.

Acknowledgements

This paper is supported by Indonesia Endowment Fund for Education (LPDP/Lembaga Pengelola Dana Pendidikan) through Pendanaan Riset Inovatif Produk (Rispro) Invitasi grant no. PRJ-6/LPDP/2020.

References

1) K.M. Abraham, "Prospects and limits of energy storage in batteries," *J. Phys. Chem. Lett.*, **6** (*5*) 830–844 (2015). doi:10.1021/jz5026273.
2) Y. Bai, N. Muralidharan, Y.K. Sun, S. Passerini, M. Stanley Whittingham, and I. Belharouak, "Energy and environmental aspects in recycling lithium-ion batteries: concept of battery identity global passport," *Mater. Today*, **41** (*December*) 304–315 (2020). doi:10.1016/j.mattod.2020.09.001.
3) K. Chihara, M. Ito, A. Kitajou, and S. Okada, "Cathode property of na _ 2c _ xo _ x [x = 4 , 5 , and 6] and k _ 2c _ 6o _ 6 for sodium-ion batteries," *Evergreen*, **4** (*1*) 1–5 (2017). doi:10.5109/1808304
4) J.P. Pender, G. Jha, D.H. Youn, J.M. Ziegler, I. Andoni, E.J. Choi, A. Heller, B.S. Dunn, P.S. Weiss, R.M. Penner, and C.B. Mullins, "Electrode degradation in lithium-ion batteries," *ACS Nano*, **14** (*2*) 1243–1295 (2020). doi:10.1021/acsnano.9b04365.
5) H. Yamada, T.S. Suzuki, T. Uchikoshi, M. Hozumi, T. Saito, and Y. Sakka, "Ideal design of textured licoo2 sintered electrode for li-ion secondary battery," *APL Mater.*, **1** (*4*) (2013). doi:10.1063/1.4824042.
6) H. Widiyandari, A.N. Sukmawati, H. Sutanto, C. Yudha, and A. Purwanto, "Synthesis of lini0.8mn0.1co0.1o2 cathode material by hydrothermal method for high energy density lithium ion battery," *J. Phys. Conf. Ser.*, **1153** (*1*) 0–7 (2019). doi:10.1088/1742-6596/1153/1/012074.
7) N. Nitta, F. Wu, J.T. Lee, and G. Yushin, "Li-ion battery materials: present and future," *Mater. Today*, **18** (*5*) 252–264 (2015). doi:10.1016/j.mattod.2014.10.040.
8) G.E. Blomgren, "The development and future of lithium ion batteries," *J. Electrochem. Soc.*, **164** (*1*) A5019–A5025 (2017). doi:10.1149/2.0251701jes.
9) R. Jung, M. Metzger, F. Maglia, C. Stinner, and H.A. Gasteiger, " Oxygen release and its effect on the cycling stability of lini x mn y co z o 2 (nmc) cathode materials for li-ion batteries ," *J. Electrochem. Soc.*, **164** (*7*) A1361–A1377 (2017). doi:10.1149/2.0021707jes.
10) J.V. Laveda, J.E. Low, F. Pagani, E. Stilp, S. Dilger, V. Baran, M. Heere, and C. Battaglia, "Stabilizing capacity retention in nmc811/graphite full cells via tmspi electrolyte additives," *ACS Appl. Energy Mater.*, **2** (*10*) 7036–7044 (2019). doi:10.1021/acsaem.9b00727.
11) B. Wang, H. Min, W. Sun, and Y. Yu, "Research on

optimal charging of power lithium-ion batteries in wide temperature range based on variable weighting factors," *Energies*, **14** (*6*) (2021). doi:10.3390/en14061776.

12) H. Sun, J. Wang, Q. Liu, Y. Zhang, D. Zhang, Q. Wang, Z. Li, W. Li, and B. Wang, "Ag–sn dual-modified lini0.8co0.1mn0.1o2 as cathode for lithium storage," *J. Alloys Compd.*, **850** 1–11 (2021). doi:10.1016/j.jallcom.2020.156763.
13) H. Lu, H. Zhou, A.M. Svensson, A. Fossdal, E. Sheridan, S. Lu, and F. Vullum-Bruer, "High capacity li[ni0.8co0.1mn0.1]o 2 synthesized by sol-gel and co-precipitation methods as cathode materials for lithium-ion batteries," *Solid State Ionics*, **249**–**250** 105–111 (2013). doi:10.1016/j.ssi.2013.07.023.
14) L. Spiridigliozzi, G. Dell'agli, M. Biesuz, V.M. Sglavo, and M. Pansini, "Effect of the precipitating agent on the synthesis and sintering behavior of 20 mol % sm-doped ceria," *Adv. Mater. Sci. Eng.*, **2016** (2016). doi:10.1155/2016/6096123.
15) D. Wang, I. Belharouak, G. Zhou, and K. Amine, "Synthesis of lithium and manganese-rich cathode materials via an oxalate co-precipitation method," *J. Electrochem. Soc.*, **160** (*5*) A3108–A3112 (2013). doi:10.1149/2.016305jes.
16) B. Xie, A. Kitajou, S. Okada, W. Kobayashi, M. Okada, and T. Takahara, "Cathode properties of na3mpo4co3 (m = co/ni) prepared by a hydrothermal method for na-ion batteries," *Evergreen*, **6** (*4*) 262–266 (2019). doi:10.5109/2547345.
17) H. Dong, and G.M. Koenig, "A review on synthesis and engineering of crystal precursors produced: via coprecipitation for multicomponent lithium-ion battery cathode materials," *CrystEngComm*, **22** (*9*) 1514–1530 (2020). doi:10.1039/c9ce00679f.
18) A.K. Pradhan, K. Zhang, R. Mundle, M. Arslan, O. Amponsah, and M. Bahoura, "Synthesis and characterization of lithium ion batteries," *Nanosensors, Biosensors, Info-Tech Sensors Syst. 2012*, **8344** 83441L (2012). doi:10.1117/12.914537.
19) A.R. Nurohmah, C.S. Yudha, M. Rahmawati, S.F.S. Nisa, A. Jumari, H. Widiyandari, and A. Purwanto, "Structural and electrochemical analysis of iron doping in lini0.6-xmn0.2co0.2fexo2 battery," *Evergreen*, **8** (*1*) 82–88 (2021). doi:10.5109/4372263.
20) J. Li, L.E. Downie, L. Ma, W. Qiu, and J.R. Dahn, " Study of the failure mechanisms of lini 0.8 mn 0.1 co 0.1 o 2 cathode material for lithium ion batteries ," *J. Electrochem. Soc.*, **162** (*7*) A1401–A1408 (2015). doi:10.1149/2.1011507jes.
21) M. Sathiya, K. Hemalatha. K. Ramesha, J.M. Tarascon, and A.S. Prakash, "Synthesis, structure and electrochemical properties of the layered sodium insertion cathode material : NaNi1/3Mn1/3Co1/3O2," *Chem. Mater*, **24** (10) 1846-1853 (2012). doi: 10.1021/cm300466b.
22) A. Jihad, A.A.N. Pratama, C.S. Yudha, M. Rahmawati, H. Widiyandari, and A. Purwanto, "Effect of zn, cu and mg doping on the structural characteristic of lini0.6mn0.2co0.2o2 (nmc622)," *ACM Int. Conf. Proceeding Ser.*, **2** 0–6 (2020). doi:10.1145/3429789.3429857.
23) S.S. Nisa, M. Rahmawati, C.S. Yudha, H. Nilasary, H. Nursukatmo, H.S. Oktaviano, S.U. Muzayanha, and A. Purwanto, "Fast approach to obtain layered transition-metal cathode material for rechargeable batteries," *Batteries*, **8** (1) 4 (2022). doi:10.3390/batteries8010004.
24) M. Ubaidullah, A.M. Al-Enizi, S. Shaikh, M.A. Ghanem, and R.S. Mane, "Waste pet plastic derived zno@nmc nanocomposite via mof-5 construction for hydrogen and oxygen evolution reactions," *J. King Saud Univ. - Sci.*, **32** (*4*) 2397–2405 (2020). doi:10.1016/j.jksus.2020.03.025.
25) S. Maeng, Y. Chung, S. Min, and Y. Shin, "Enhanced mechanical strength and electrochemical performance of core–shell structured high–nickel cathode material," *J. Power Sources*, **448** 227395 (2020). doi:10.1016/j.jpowsour.2019.227395.
26) N.N. Sinha, and N. Munichandraiah, "The effect of particle size on performance of cathode materials of li-ion batteries," *J. Indian Inst. Sci.*, **89** (*4*) 381–392 (2009).
27) C.S. Yudha, S.U. Muzayanha, W. Hendri, F. Iskandar, W. Sutopo, A. Purwanto, H. Widiyandari, F. Iskandar, W. Sutopo, and A. Purwanto, "Synthesis of lini0.85co0.14al0.01o2 cathode material and its performance in an nca / graphite full-battery," *Energies*, **12** (*1886*) 1886 (2019). doi:10.3390/en12101886
28) N. Zhang, J. Li, H. Li, A. Liu, Q. Huang, L. Ma, Y. Li, and J.R. Dahn, "Structural, electrochemical, and thermal properties of nickel-rich lini x mn y co z o 2 materials," *Chem. Mater.*, **30** (*24*) 8852–8860 (2018). doi:10.1021/acs.chemmater.8b03827.
29) F. Yang, D. Wang, Y. Zhao, K.L. Tsui, and S.J. Bae, "A study of the relationship between coulombic efficiency and capacity degradation of commercial lithium-ion batteries," *Energy*, **145** 486–495 (2018). doi:10.1016/j.energy.2017.12.144.